2018 European Control Conference (ECC)
June 12-15, 2018. Limassol, Cyprus

Real-Time Optimal Trajectory Generation for a Quadrotor UAV on the Longitudinal Plane

Bruno Carvalho*, Michael Di Perna†, Luis Rodrigues‡
Department of Electrical and Computer Engineering
Concordia University, Montreal, Canada
Email: *b_per@encs.concordia.ca, †m_dipern@encs.concordia.ca, ‡luisrod@encs.concordia.ca

***Abstract*—This paper presents an optimal real-time Flight Management System (FMS) for quadrotor Unmanned Aerial Vehicles (UAVs) which minimizes a trade-off between costs associated with body acceleration and total time. The contribution of this paper is an optimal state feedback solution that considers the nonlinearities of the quadrotor's equations of motion. This solution is derived using the Pontryagin's Minimum Principle (PMP). Several simulations are presented including a plot of the Pareto optimal curve yielding a trade-off between the energy of the acceleration and the flight time.**

I. Introduction

A quadrotor UAV is a class of rotorcraft characterized by a configuration of four propellers positioned in such a way that a pair of rotors counter balance the torque of the opposite pair. Position, and yaw can be controlled by changing the thrust of each propeller. Due to their versatility, quadrotors have been used in several fields in recent years. Applications can vary from aerial mapping, traffic and agricultural surveillance, to rescue operations, to name a few. The first part of any UAV mission is the path generation or trajectory planning task, which is can be performed by a FMS [1]-[3]. The formulation of the trajectory planning problem for UAVs has evolved from the simple shortest path approach to complex optimization problems, such as, minimum time [4]-[7], minimum snap [8], minimum derivatives [9], among others. Dynamic programming [10], Model Predictive Control (MPC) [11], and genetic algorithms [6][12], have been proposed to address signal constraints and feasibility [9], collision avoidance [13], nonlinearities [14], and multiple vehicle formation [13][15].

Trajectory generation for UAVs based on energy-related criteria has not been vastly addressed in the literature. A heuristic procedure is proposed in [16] to solve the Generalized Traveling Salesman Problem with Neighbourhoods (TSPN) addressing the energy consumption problem of a six-rotor aircraft. Reference [17] sets up an optimal control problem for car-like robots in order to find paths and velocity profiles that minimize the energy consumed during motion. Similarly, [18] determines minimum-energy trajectories for a quadrotor solving numerically an optimal control problem for angular accelerations of the propellers. Reference [19] proposes an adaptive mission planner by solving numerically a Mixed Integer Linear Programming (MILP) to estimate the available energy for the quadrotor mission.

Motivated by the energy efficiency issue, the present work proposes a methodology for determining the optimal trajectories of a quadrotor in the sense of a trade-off between a cost associated with the body acceleration and a time-related cost. The problem is formulated as a free terminal time optimal control problem [20] using a trade-off cost index C_I. In order to handle the nonlinearities of the system, this paper proposes a change of variables that leads to a linear formulation of the two point boundary value problem. After the linear problem is solved the inverse transformation of variables yields the final solution. The main advantage of this technique is that it provides a state-feedback analytical expression, which is a key feature for real-time trajectory replanning, especially considering limited on-board CPU capabilities for small vehicles.

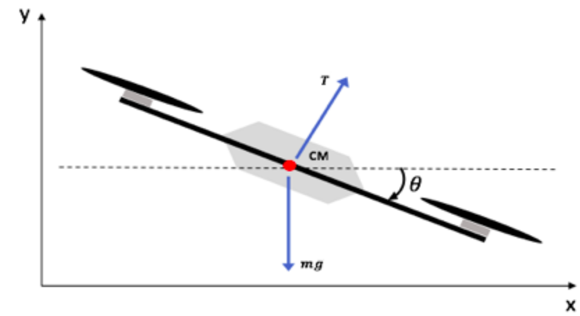

Figure 1. Quadrotor free body diagram and pitch angle convention.

The paper is organized as follows. The optimal control problem formulation and the stated assumptions are presented in Section II. Section III describes the proposed trajectory generation methodology using the PMP [21]. Section IV is dedicated to simulation results. Conclusions are drawn in Section V.

II. Problem Formulation

The objective of this work is to design trajectories for a quadrotor starting at a given position and arriving with zero speed at a target point, which can be the origin without loss of generality. The following assumptions are made:
1) The quadrotor is a rigid body.
2) Yaw is considered constant for longitudinal trajectories.
3) The ground effect can be neglected at the flying altitude.

The forces acting on the quadrotor are illustrated in Figure

(1). Ignoring drag, the translational equations of motion in the x-y plane are

$$m\ddot{x} = Tsin(\theta), \quad m\ddot{y} = Tcos(\theta) - mg \tag{1}$$

where θ is the pitch angle, considered to be positive clockwise, g is the gravitational constant, T is the total propeller thrust, and m is the quadrotor weight. Rewriting (1) considering the horizontal and vertical accelerations as control inputs leads to

$$u_1 = \ddot{x} = \frac{T}{m}sin(\theta), \quad u_2 = \ddot{y} = \frac{T}{m}cos(\theta) - g, \tag{2}$$

respectively. The quadrotor's position is described by x and y and its velocity by v_x and v_y. Position and velocities form the state vector $\mathbf{x} = [x \;\; y \;\; v_x \;\; v_y]^T$.

The optimal control problem for trajectory generation can be stated as

$$\min_{\mathbf{u},t_f} \int_0^{t_f} \left(\frac{1}{2}\mathbf{u}^T\mathbf{u} + C_I\right) d\tau \tag{3}$$

$$subject\ to\ (2),\ \mathbf{x}(0) = \mathbf{x_0},\ \mathbf{x}(t_f) = \mathbf{x_f} \tag{4}$$

where $\mathbf{x_0}^T = [x_0 \; y_0 \; v_{x_0} \; v_{y0}], \mathbf{x_f}^T = [0 \; 0 \; 0 \; 0]$, $\mathbf{u}^T = [u_1 \; u_2]$, and C_I is the trade-off coefficient between costs associated with body acceleration and total flight time. The higher the value of C_I the higher is the weight on the total flight time.

III. Problem Solution

Theorem 1. *Assume that $C_I > 0$ is given. Then the solution to the optimal control problem (3)–(4) is*

$$\theta^* = \begin{cases} tan^{-1}\left(\frac{u_1^*}{u_2^*+g}\right), & u_2^* \neq -g \\ \pi/2, & u_2^* = -g, u_1^* > 0 \\ -\pi/2, & u_2^* = -g, u_1^* < 0 \end{cases}$$
$$T^* = \begin{cases} \frac{m(u_2^*+g)}{cos(\theta^*)}, & \theta^* \neq \pm\pi/2 \\ m\ u_1^*, & \theta^* = \pi/2 \\ -m\ u_1^*, & \theta^* = -\pi/2 \end{cases} \tag{5}$$

with $\theta^* \in [-\pi/2, \pi/2]$, where

$$\begin{bmatrix} u_1^{*2} \\ u_2^{*2} \end{bmatrix} = \begin{bmatrix} 2(C_I + J_x v_x + J_y v_{y0}) - J_{v_y}^2(0) \\ 2(C_I + J_y v_y + J_x v_{x0}) - J_{v_x}^2(0) \end{bmatrix} \tag{6}$$

and the costate variables are given by

$$J_x = \frac{6(2x_0 + v_{x0}t_f)}{t_f^3},\ J_y = \frac{6(2y_0 + v_{y0}t_f)}{t_f^3},$$
$$J_{v_x}(0) = \frac{2(3x_0 + 2v_{x0}t_f)}{t_f^2},\ J_{v_y}(0) = \frac{2(3y_0 + 2v_{y0}t_f)}{t_f^2}. \tag{7}$$

Proof: Let the cost-to-go be defined as

$$J = \int_t^{t_f} \left(\frac{1}{2}\mathbf{u}^T\mathbf{u} + C_I\right) d\tau \tag{8}$$

The Hamiltonian of the system is

$$H = \frac{1}{2}u_1^2 + \frac{1}{2}u_2^2 + C_I + J_x v_x + J_{v_x}u_1 + J_y v_y + J_{v_y}u_2 \tag{9}$$

A necessary condition for optimality is $H_{u_1} = H_{u_2} = 0$ (where H_u is the partial derivative of H with respect to u) which yields

$$u_1^* = -J_{v_x}, \quad u_2^* = -J_{v_y} \tag{10}$$

Therefore, from the dynamics (2) we have

$$J_{v_x} = -\dot{v}_x, \quad J_{v_y} = -\dot{v}_y \tag{11}$$

From the Hessian matrix of H with respect to u_1 and u_2 we get the Legendre-Clebsch sufficient condition of optimality

$$\begin{bmatrix} H_{u_1u_1} & H_{u_1u_2} \\ H_{u_2u_1} & H_{u_2u_2} \end{bmatrix} = \begin{bmatrix} 1 & 0 \\ 0 & 1 \end{bmatrix} > 0 \tag{12}$$

There are no penalties associated with final states in our cost functional. Therefore according to the transversality equations $H(t_f) = 0$. Additionally, the final time is considered to be free, and the Hamiltonian does not depend explicitly on time, which together with $H(t_f) = 0$ makes $\dot{H}(t) = 0$ and $H^* \equiv 0$ [22]. Replacing u_1^* and u_2^* from (10) in the system's Hamiltonian (9) results in

$$J_{v_x}^2 + J_{v_y}^2 = 2(C_I + J_x v_x + J_y v_y) \tag{13}$$

According to PMP and Hamilton's equations [21], [22]

$$\begin{bmatrix} \dot{J}_x \\ \dot{J}_{v_x} \\ \dot{J}_y \\ \dot{J}_{v_y} \end{bmatrix} = \begin{bmatrix} 0 \\ -J_x \\ 0 \\ -J_y \end{bmatrix} \tag{14}$$

Consequently, J_x and J_y are constant in time and J_{v_x} and J_{v_y} are linear functions that can be written in the form

$$\begin{aligned} J_{v_x}(t) &= -J_x t + J_{v_x}(0) \\ J_{v_y}(t) &= -J_y t + J_{v_y}(0) \end{aligned} \tag{15}$$

Having (15), one can integrate (11) to find expressions for $v_x(t)$ and $v_y(t)$.

$$\begin{aligned} v_x(t) &= -\int_0^t J_{v_x}(\tau)d\tau + v_x(0) = \frac{J_x t^2}{2} - J_{v_x}(0)t + v_x(0) \\ v_y(t) &= -\int_0^t J_{v_y}(\tau)d\tau + v_y(0) = \frac{J_y t^2}{2} - J_{v_y}(0)t + v_y(0) \end{aligned} \tag{16}$$

Integrating (16) yields

$$\begin{aligned} x(t) &= \int_0^t v_x(\tau)d\tau + x(0) = \frac{J_x t^3}{6} - \frac{J_{v_x}(0)t^2}{2} + v_{x0}t + x(0) \\ y(t) &= \int_0^t v_y(\tau)d\tau + y(0) = \frac{J_y t^3}{6} - \frac{J_{v_y}(0)t^2}{2} + v_{y0}t + y(0) \end{aligned} \tag{17}$$

It is possible to replace the expressions (15) and (16) into the system Hamiltonian equation described in (13) to obtain

$$J_{v_x}^2 = 2(C_I + J_x v_x + J_y v_{y0}) - J_{v_y}^2(0) \tag{18}$$

Using (10) equation (18) reduces to

$$u_1^* = \pm\sqrt{2(C_I + J_x v_x + J_y v_{y0}) - J_{v_y}^2(0)} \tag{19}$$

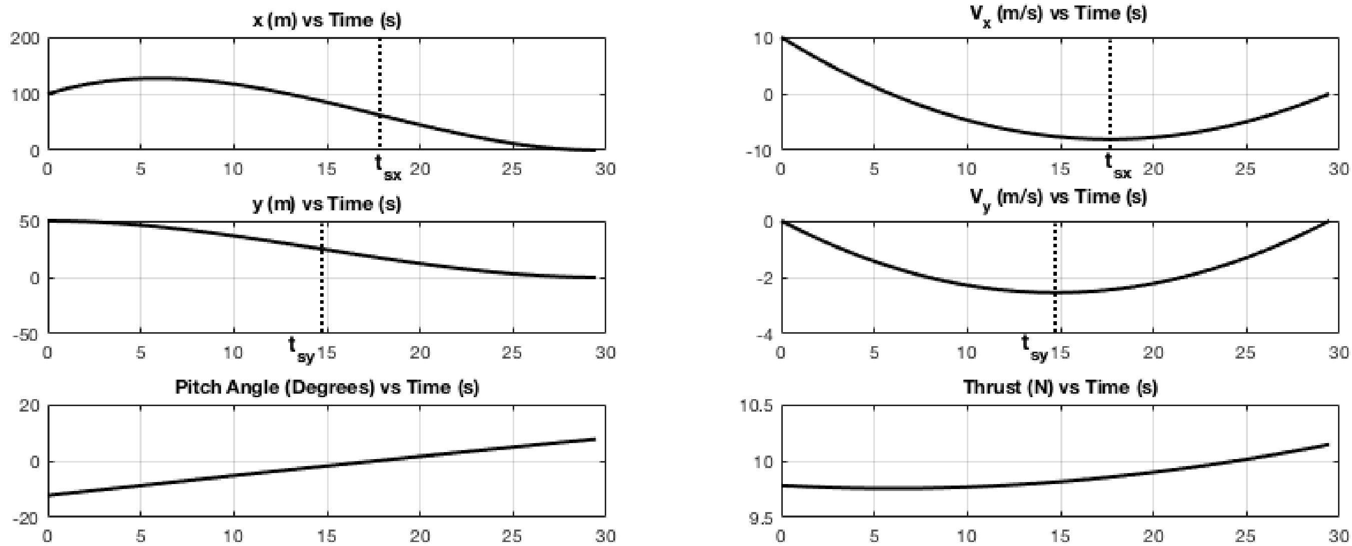

Figure 2. Optimal trajectories.

and u_2^* is obtained similarly as

$$u_2^* = \pm\sqrt{2(C_I + J_y v_y + J_x v_{x_0}) - J_{v_x}^2(0)} \tag{20}$$

The system of equation formed by (13), (16), and (17) at the final time can be solved for the unknowns J_x, J_v, $J_{v_x}(0)$, $J_{v_y}(0)$, and t_f. Doing this, the final time t_f is a real positive root of the quartic polynomial

$$C_I t_f^4 - 2(v_{x_0}^2 + v_{y_0}^2)t_f^2 - 12(v_{x_0}x_0 + v_{y_0}y_0)t_f - 18(x_0^2 + y_0^2) = 0 \tag{21}$$

In this case, because the zero and second order terms are negative, there are at least two real roots and according to the Descartes' rule of signs one of those roots is positive. The remaining unknowns for the general solution can then be obtained by the solution of the system of linear equations (16) and (17) evaluated at the final time, which yields (7). The results can be replaced back into equations (17) and (16) in order to get expressions for $x(t)$, $y(t)$, $v_x(t)$, and $v_y(t)$. Finally, the thrust profile and pitch angle can then be obtained by inverting the change of input coordinates in equations (2), which finishes the proof. ∎

Remark 1. *Given a specific C_I, it is possible to determine the optimal inputs u_1^* and u_2^* knowing the velocity states (v_x, v_y) and initial conditions (x_0, y_0, v_{x_0}, v_{y_0}).*

Remark 2. *For the special case in which the quadrotor is initially at zero speed ($v_{x_0} = 0$ and $v_{y_0} = 0$) the final time is*

$$t_f = \left(\frac{18(x_0^2 + y_0^2)}{C_I}\right)^{\frac{1}{4}} \tag{22}$$

Corollary 1.1. *Assume $x_0 > 0$ and $y_0 > 0$, then the optimal control law that achieves the state (0, 0, 0, 0) is given by the state feedback form*

$$u_1^* = \begin{cases} -\sqrt{2(C_I + J_x v_x + J_y v_{y_0}) - J_{v_y}^2(0)}, & t < t_{s_x} \\ 0, & t = t_{s_x} \\ +\sqrt{2(C_I + J_x v_x + J_y v_{y_0}) - J_{v_y}^2(0)}, & t > t_{s_x} \end{cases}$$
$$u_2^* = \begin{cases} -\sqrt{2(C_I + J_y v_y + J_x v_{x_0}) - J_{v_x}^2(0)}, & t < t_{s_y} \\ 0, & t = t_{s_y} \\ +\sqrt{2(C_I + J_y v_y + J_x v_{x_0}) - J_{v_x}^2(0)}, & t > t_{s_y} \end{cases} \tag{23}$$

where the switching times occur at

$$t_{s_x} = \frac{(3x_0 + 2v_{x_0}t_f)t_f}{6x_0 + 3v_{x_0}t_f}, \; t_{s_y} = \frac{(3y_0 + 2v_{y_0}t_f)t_f}{6y_0 + 3v_{y_0}t_f} \tag{24}$$

Proof: The switching time of u_1^* occurs when the acceleration along the x axis is zero, meaning from equation (11) that $J_{v_x}(t_{s_x}) = 0$, or similarly, from equation (15), that

$$t_{s_x} = J_{v_x}(0)/J_x. \tag{25}$$

Equations (7) can then be replaced into (25) to yield (24). Repeating this procedure for y finishes the proof. ∎

Remark 3. *If the quadrotor is initially at zero speed, the switching time of each coordinate is equal to $t_f/2$.*

Remark 4. *Since the pitch angle was considered as an input, it is important to note that the generated optimal trajectories allow pitch discontinuities. However, this simplification has very low impact on the overall performance since the solution is interpreted as a trajectory reference for the trajectory-tracking controller that will then smooth out the dynamic response in closed-loop.*

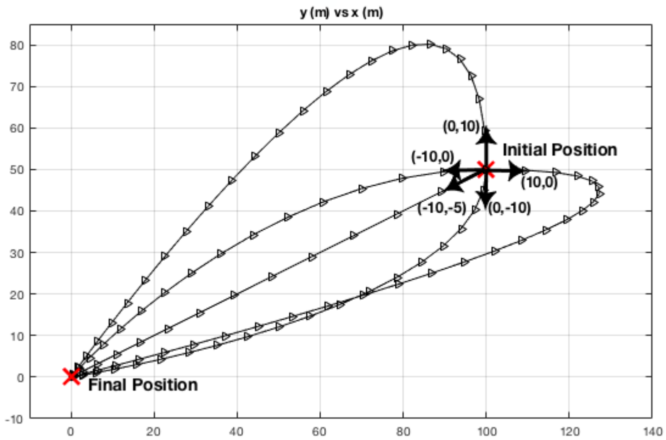

Figure 3. Optimal Paths.

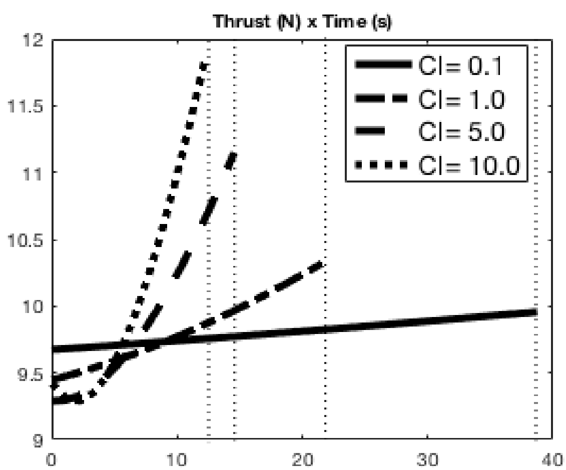

Figure 4. Thrust Profile for different Cost Indices.

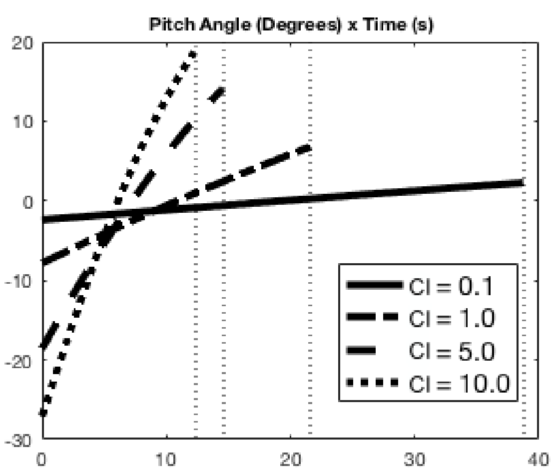

Figure 5. Pitch Angle for different Cost Indices.

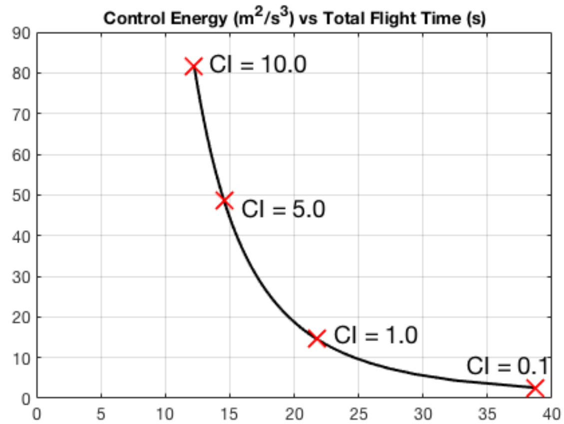

Figure 6. Pareto-optimal trade-off curve.

IV. SIMULATION RESULTS

This section presents the results of simulation for the solution discussed in the previous sections. The Ascending Technologies AscTec Hummingbird quadrotor parameters were adopted according to [26] in which $m = 0.71\ Kg$. Additionally, $g = 9.81 m/s^2$. For simulation purposes the quadrotor's initial state is considered to be $(x_0, y_0, v_{x_0}, v_{y_0}) = (100, 50, 10, 0)$, the trade-off coefficient ($C_I = 1$), and no drag is considered. Figure 2 shows the optimal trajectories for position, velocity, pitch angle and thrust. The final time obtained in the simulation was 29.45 seconds. Because $v_{y_0} = 0\ m/s$, the switching time for the coordinate y occurs exactly at the half point of the flight time. On the other hand, because $v_{x_0} = -10\ m/s$ the switching time for the coordinate x occurs later at t = 17.64 seconds. As predicted, the resulting pitch angle profile contains discontinuities at initial and final states.

Figure 3 illustrates optimal trajectories for quadrotors starting at the same position but with different initial velocities. The interval between two consecutive marks represents 1 second. The initial velocity vectors are represented by arrows. As expected, trajectories in which the initial velocities are unfavorable to move in the direction of the final target take longer than the trajectories with favorable initial conditions. The optimal path becomes a straight line if the initial velocity vector $\boldsymbol{v_0} = (v_{x_0}, v_{y_0})$ can be written as $\boldsymbol{v_0} = c\ \boldsymbol{x_0}$ where c is a real scalar and $\boldsymbol{x_0}$ is the initial position vector. The parameter C_I allows tuning the trajectories of the system based on a trade-off between the energy of the acceleration and the flight time. Figure 4 shows the influence of C_I on the thrust profile in the case where $(x_0, y_0, v_{x_0}, v_{y_0}) = (100, 50, 0, 0)$. As expected, higher cost indices provide shorter flight times but require a higher thrust. The pitch angle is shown in figure 5 considering the same initial conditions. It can be seen that higher cost indices require more aggressive maneuvers (larger pitch angles).

The Pareto-optimal trade-off curve between the total flight time and the amount of control energy required for different values of C_I is shown in figure 6. From this plot, it is possible to conclude that if the cost index increases the total flight time decreases and the energy of the acceleration increases.

V. Conclusion

This paper presented and analyzed an optimal trajectory generation algorithm for quadrotors. The main advantage of the proposed method is the analytical feedback solution that allows real-time implementation on devices with limited onboard CPU capabilities. The methodology can also handle system nonlinearities. Results from simulations show how a coefficient can be used to trade-off the energy of the acceleration versus flight time, as well as to guarantee that the maximum thrust constraint is met.

VI. Acknowledgements

The authors would like to acknowledge the National Sciences and Engineering Research Council (NSERC), the Mathematics of Information Technology and Complex Systems (MITACS), and Echoer Canada Inc. for funding this research.

References

[1] T. Rivers, Design and Integration of a Flight Management System for the Unmanned Air Vehicle Frog, Master thesis. Naval Postgraduate School, Monterey, 1998.

[2] K. Eliker, H. Bouadi, and M. Haddad, Flight Planning and Guidance Features for an UAV Flight Management Computer Ecole Militaire Polytechnique. IEEE Emerging Technologies and Factory Automation (ETFA), 2016.

[3] A. Tarhan, et al., Formal intent based Flight Management System design for unmanned aerial vehicles, Controls & Istanbul Tech. IEEE Unmanned Aircraft Systems (ICUAS), 2014.

[4] Y. Bouktir, M. Haddad, and T. Chettibi, Trajectory planning for a quadrotor helicopter, 16th Mediterranean Conference on Control and Automation. IEEE. 2008.

[5] M. Hehn and R. D'Andrea, Real-Time Trajectory Generation for Quadrocopters, Institute for Dynamic Systems and Control, ETH Zurich. IEEE Transactions on Robotics, 2015.

[6] C. C. Yang, L.C. Lai, and C. J. Wu, Time-optimal control of a hovering quadrotor helicopter, IEEE Int. Conf. on Syst. & Signals. IEEE-ICSS, pp295-300, 2005.

[7] R. Ritz, et al., Quadrocopter Performance Benchmarking Using Optimal Control, in Proc. Int. Conf. Intelligent Robots and Systems. San Francisco, CA, 2011.

[8] D. Mellinger and V. Kumar, Minimum Snap Trajectory Generation and Control for Quadrotors, IEEE International Conference on Robotics and Automation. Shanghai, 2011.

[9] C. Richter, A. Bry, and N. Roy Polynomial Trajectory Planning for Aggressive Quadrotor Flight in Dense Indoor Environments, Massachusetts Institute of Technology. ISRR, 2013.

[10] I. Palunko, R. Fierro, and P. Cruz, Trajectory generation for swing-free maneuvers of a quadrotor with suspended payload: A dynamic programming approach, International Conference on Robotics and Automation. Pages 2691-2697, May 2012.

[11] L. Singh, J. Fuller, Trajectory generation for a UAV in urban terrain, using nonlinear MPC, IEEE American Control Conference. IEEE, 2001.

[12] V. Roberge, M. Tarbouchi, and G. Labonte, Comparison of Parallel Genetic Algorithm and Particle Swarm Optimization for Real-Time UAV Path Planning, IEEE International Conference on Robotics and Automation. Volume: 9, Issue: 1, Feb. 2013.

[13] V. Chichella, et al., Safe Coordinated Maneuvering of Teams of Multirotor Unmanned AerialVehicles, IEEE Control Systems, Vol 36, Number 4. Pages 59-82, 2016.

[14] M. Geisert and N. Mansard, Trajectory Generation for Quadrotor Based Systems using Numerical Optimal Control, International Conference on Robotics and Automation. Sweden, 2016.

[15] E. Xargay, et al., Time-Critical Cooperative Control of Multiple Autonomous Vehicles, IEEE Control Systems, Vol 32, Number 5. Pages 49-73, 2012.

[16] K. Vicencio, T. Korras, and K. Bordigon, Energy-optimal path planning for six-rotors on multi-target missions, Intelligent Robots and Systems (IROS). IEEE, 2015.

[17] P. Tokekar, N. Karnad, and V. Isler, Energy-optimal trajectory planning for car-like robots, Journal Autonomous Robots archive (Volume 37 Issue 3). Hingham, 2014.

[18] F. Morbidi, R. Cano, and D. Lara, Minimum-Energy Path Generation for a Quadrotor UAV, IEEE International Conference on Robotics and Automation. Stockholm, 2016.

[19] A. Candido, R. Galvao, and T. Yoneyama, Control and energy management for quadrotor, ICC. UK, 2014, pp. 343-348.

[20] A. E. Bryson and Y. Ho, Applied Optimal Control Blaisdell Publishing Company, 1983.

[21] L. Pontryagin, et al.,The Mathematical Theory of Optimal Processes 4th ed. Nauka. Blaisdell Moscow, 1983.

[22] D. Liberzon, Calculus of Variations and Optimal Control Theory: A concise Introduction, ISBN 978-0-691-15187-8. Princeton University Press, 2012.

[23] R. Mahony, V. Kumar and P, Corke, Multirotor Aerial Vehicles: Modeling, Estimation, and Control of Qua- drotor. Robotics. Automation Magazine, 2012.

[24] R. Gill, R. D'Andrea and P, Corke, Propeller Thrust and Drag in Forward Flight, IEEE Conference on Control Technology and Applications (CCTA). Hawaii, 2017.

[25] T. Luukkonen, Modelling and control of quadcopter, Aalto University School of Science. Espoo, 2011.

[26] Ascending Technologies. Technical Data - AscTec Hummingbird. Ascending Technologies. webpage available online from: http://www.asctec.de/en/uav-uas-drones-rpas-roav/asctec-hummingbird/.